Available online at ScienceDirect

Resuscitation

journal homepage: www.elsevier.com/locate/resuscitation

Original paper

Prediction of survival after pediatric cardiac arrest using heart rate variability and machine learning

Daishi Xu[a], *Eris van Twist*[b], *Marit Verboom*[c], *Maayke Hunfeld*[b,c], *Corinne Buysse*[c], *Geurt Jongbloed*[d], *Natasja M.S. de Groot*[a], *Robert van den Berg*[c,*]

Abstract

Background: Early prognostication of the outcome in pediatric cardiac arrest (CA) patients is crucial for clinical decision-making. Heart rate variability (HRV) has shown potential in predicting outcomes after CA in adult patients. This study investigates whether HRV can be used to predict survival outcomes after pediatric CA using machine learning techniques.

Methods: This retrospective study included children with CA, who achieved return of spontaneous circulation (ROSC), and were admitted to the pediatric intensive care unit (PICU) of a tertiary hospital between 2012 and 2021. A 5-min electrocardiogram (ECG) segment acquired at 24 h after CA was used to calculate HRV parameters (time-, frequency-, and non-linear domains). These parameters were used to train a random forest model. The primary outcome was 12-month survival or death. Model performance was evaluated using receiver-operating characteristics (ROC) analysis and predictive values. Feature importance was assessed using Shapley values.

Results: A total of 76 patients (male: 63.2%, median age: 2.5 [IQR: 0.4–8.0] years) were divided into survival (34) or death (42) groups based on 12-month outcomes. The machine learning model achieved an accuracy of 77.6% and a positive predictive value of 0.879 for mortality prediction. The most influential features for model predictions were the frequency-domain parameters total power and very-low frequency (VLF) power, with lower values associated with an increased probability of death.

Conclusions: Analysis of HRV at 24 h after ROSC may serve as a strong predictor of 12-month survival after pediatric CA.

Keywords: Pediatric cardiac arrest, Heart rate variability, Prognosis, Machine learning, Survival, Autonomic nervous system

Introduction

Annually in the United States, around 15,000 children experience in-hospital cardiac arrest (IHCA) and approximately 6000 cases experience out-of-hospital cardiac arrest (OHCA).[1,2] Developments in advanced life support technologies have contributed to improving rates of return of spontaneous circulation (ROSC). However, low survival rates (approximately 40% IHCA and 6.7–10.2% OHCA) following pediatric cardiac arrest (CA) remain a cause for concern.[3–6]

Evidence indicates that post-resuscitation brain injury is a primary cause of mortality and unfavorable outcomes among pediatric patients resuscitated from CA.[7,8] The hypoxic-ischemic injury following CA damages the cerebral cortex, insula, hippocampus, and

Abbreviations: AUC, Area Under The Receiver Operator Characteristics Curve, ANS, Autonomic Nervous System, CA, Cardiac Arrest, CPR, Cardiopulmonary Resuscitation, DFA α1, Detrended Fluctuation Analysis Over Short Time, DFA α2, Detrended Fluctuation Analysis Over Long Time, ECG, Electrocardiogram, EEG, Electroencephalogram, FDR, False Discovery Rate, HF, High Frequency, HRV, Heart Rate Variability, ICU, Intensive Care Unit, IHCA, In-Hospital Cardiac Arrest, LF, Low Frequency, Ln VLF, The Natural Logarithm Of Very-Low Frequency, pNN50, Proportion Of Adjacent RR Intervals Differing By >50 ms, OHCA, Out-Of-Hospital Cardiac Arrest, PCPC, Pediatric Cerebral Performance Category, PICU, Pediatric Intensive Care Unit, RMSSD, Root Mean Square Of Successive Differences, ROSC, Return Of Spontaneous Circulation, SD1, Standard Deviation Orthogonal To The Line Of Identity, SD2, Standard Deviation Along The Line Of Identity, SDNN, Standard Deviation Of The RR Intervals, SHAP, Shapley Additive Explanations, SSEP, Somatosensory Evoked Potentials, VIS, Vasoactive-Inotropic Score

* Corresponding author at: Department of Neurology, Erasmus Medical Center, Dr. Molewaterplein 40, 3015GD Rotterdam, the Netherlands.
E-mail address: r.vandenberg@erasmusmc.nl (R. van den Berg).

https://doi.org/10.1016/j.resuscitation.2026.110983
Received 6 October 2025; Received in Revised form 30 December 2025; Accepted 13 January 2026

brainstem, leading to neurological disability and autonomic nervous system (ANS) disruption.[9–11]

Early and accurate prediction of long-term outcomes in these children is crucial for treatment decisions but remains an unresolved issue. Consensus guidelines regarding the use of electrophysiological and radiological biomarkers for prognosis are available for adult CA survivors.[12] Multiple modalities (e.g., neurologic examination, electroencephalography (EEG)) are recommended for prognostication after pediatric CA, but the absence of standardized interpretation underscores the need for further research into pediatric outcome prediction.[13]

Following CA, early lesions in brain regions associated with the ANS are associated with high mortality.[14] Heart rate variability (HRV), the variation in intervals between consecutive heartbeats, reflects the dynamic influence of sympathetic and parasympathetic activity on heart rate. Time-, frequency- and nonlinear-domain analysis are used to quantify HRV, based on RR intervals derived from the ECG, which is widely accessible in the pediatric intensive care unit (PICU). Accordingly, HRV is widely regarded as a non-invasive indicator of ANS activity.[15] HRV is associated with prognosis of patients in the intensive care unit (ICU), with decreased variability in CA non-survivors.[16–18]

The natural logarithm of very-low frequency (ln VLF) power and detrended fluctuation analysis (DFA α1) are significantly associated with unfavorable outcomes in CA patients.[19] Additionally, normalized low-frequency power (LFP) was identified as an independent predictor of 24-h mortality in resuscitated patients.[20] As this previous work focused on the outcomes in the adult CA population, the applicability of these HRV parameters in pediatric patients remains to be explored.

Recently, quantitative EEG combined with machine learning models has shown promising results in predicting 12-month survival in children following CA.[21] However, machine learning models incorporating HRV features derived from ECG have not yet been applied for prognostic prediction in pediatric CA patients. This study aims to develop an explainable machine learning model using HRV features for predicting long-term outcomes in pediatric CA patients, thereby providing clinical insights into HRV after pediatric CA and supporting individualized clinical decision-making.

Methods

Study design

This retrospective study was conducted at the Erasmus MC Sophia Children's Hospital in Rotterdam, involving the pediatric intensive care unit (PICU) and clinical neurophysiology department. As a tertiary care university hospital, it provides health care to children of the southwest Netherlands. This region has approximately 4 million inhabitants, which accounts for about 25% of the Dutch population. The study (MEC-2019-0259 and MEC-2021-0145) was approved by the Erasmus MC Ethical Review Board. The requirement for informed consent from patients was waived.

Patient inclusion

The study population included children (0–17 years) with IHCA or OHCA between 2012 and 2021 who were admitted to the PICU after ROSC and monitored using EEG at 24 h after CA. CA was defined as documented unresponsiveness with absent pulse $\geq$1 min. Exclusion criteria included: (1) preexisting severe neurologic deficits, defined as a prearrest Pediatric Cerebral Performance Category (PCPC) score of >3; (2) traumatic OHCA; or (3) intracranial lesions such as intracranial hemorrhage, brain tumor, or meningitis as a cause of arrest.

Outcomes

The primary outcome is consistent with our previous study, dichotomized as survival (PCPC 1–5) or death (PCPC 6) at 12 months after CA. The PCPC scores were obtained through our multidisciplinary follow-up program at 12 months after CA, which is assessed by an experienced pediatric intensivist (C.B.) and pediatric neurologist (M.H.). For patients without follow-up, outcomes were extracted from patient records (e.g., records from hospital visits with other physicians).

ECG registration and preprocessing

A single-lead ECG was recorded using an OSG BrainRT system (Rumst, Belgium) at a 250 or 256 Hz sampling rate. A continuous 5-min segment was extracted from the recordings at exactly 24 h following CA. ECG segments with non-sinus rhythm were excluded from the analysis. HRV is assessed from RR interval extracted by identifying the R-peaks in QRS complexes.[15]

R-peaks detection was performed in python 3.11 using the BioSPPy toolbox.[22] Following this identification, RR intervals were subsequently calculated. RR intervals from any ectopic beats and inaccuracies in R-peak detection (incorrectly detected or missed R-peaks due to noise or artifacts) were visually inspected and manually removed. Corrections were applied to the RR interval time series using linear interpolation techniques to address discrepancies resulting from the exclusion of these anomalies.[15] Patients with removal of more than 20% of RR intervals were excluded.

HRV parameters

HRV was calculated from the ECG at 24 h after CA using time-domain, frequency-domain, and nonlinear analysis approaches. Time-domain analysis included SDNN (standard deviation of normal RR intervals); RMSSD (root mean square of successive RR interval differences); and pNN50 (proportion of adjacent RR intervals differing by >50 ms). Frequency-domain analysis included the power spectral density calculated for the very low frequency (VLF, 0.003–0.04 Hz), low frequency (LF, 0.04–0.15 Hz), and high frequency (HF, 0.15–0.4 Hz) bands.[15] The power was calculated for the total signal, and within each frequency band as absolute power and relative to total power. For LF and HF bands, normalized powers and the LF/HF ratio were calculated. Nonlinear analysis included the standard deviation orthogonal to the line of identity (SD1), the standard deviation along the line of identity (SD2), and their ratio (SD2/SD1) derived from Poincaré plot. Sample entropy and detrended fluctuation analysis (DFA α1, DFA α2) were also performed.[23] All parameters were computed in python using pyHRV toolbox.[24]

VIS score calculation

The Vasoactive-Inotropic Score (VIS) is an assessment tool to quantify cardiovascular pharmacological support, reflecting the hemodynamic management of patients. The score is calculated based on the maximum dosage of each drug in the three hours before the first 24 h after CA. The VIS can be calculated using the formula dopamine (μg/kg/min) + dobutamine (μg/kg/min) + 100 × epinephrine (μg/kg/min) + 100 × norepinephrine (μg/kg/min) + 10 × milrinone

(μg/kg/min) + 10,000 × vasopressin (units/kg/min) + 50 × levosimendan (μg/kg/min).[25]

Random forest classifier

HRV features extracted per patient were used as input for a random forest classifier, using survival or death after 12 months as the training label. The dataset was divided into training and test sets using stratified 5-fold cross-validation (80% training/20% testing) in Python Scikit-learn.[26] Stratified sampling was applied to ensure the balance of the outcome classes between the test and training subsets. Optimal hyperparameters for the random forest model were selected using a grid search algorithm, with precision as optimization metric.

The model returned a probability estimate (ranging from 0 to 1) of an unfavorable outcome for each patient. To reduce the false positive rate, a probability threshold of 0.7 was used to classify the outcome of a patient as unfavorable. To evaluate the model performance, the area under the receiver operator characteristics curve (AUC), recall, precision, and F1-score were calculated. The F1-score was defined as 2 × [precision × recall]/[precision + recall].

We employed a Shapley Additive Explanations (SHAP, Python Shap[27]) analysis to quantify the contribution of HRV features to classification decisions. This approach enables feature importance ranking and individual decision visualization, dramatically improving model interpretability.

Statistical analyses

Continuous variables were displayed as median [interquartile range] and compared with the Mann-Whitney *U* test, and False Discovery Rate (FDR) correction applied for multiple comparisons. Categorical variables were expressed as counts (percentage) and compared using the chi-squared test, Fisher's exact test (binary variables), and the Fisher-Freeman-Halton test (multiclass variables). Statistical significance was defined as $p < 0.05$. Statistical analysis was performed using Python 3.11.

Results

Study population

Our study population consisted of a total of 459 children with CA (213 OHCA, 246 IHCA) between 2012 and 2021, of which 393 individuals (86%) achieved ROSC. Of these patients, 153 (39%) underwent EEG/ECG monitoring, with EEG/ECG raw data available. A total of 69 cases were excluded based on the pre-defined criteria, resulting in 84 eligible patients. A further 8 patients were excluded based on artifact-obscured data, non-sinus rhythm, or >20% inaccurately calculated RR intervals, resulting in 76 ECG recordings for further HRV analysis (Fig. 1).

Patient characteristics are described in Table 1. The median age of the 76 children included in the study at the time of cardiac arrest was 2.5 years, 63.2% were males. OHCA accounted for 71.1% of cases. At 12 months after CA, mortality rate was 55.3% (42/76). Most patients (35/42, 83.3%) died of neurological causes, in approximately half of the patients (20/42, 48%) a decision was taken to withdraw life-sustaining therapy. Timing and cause of death for part of this cohort are described in more detail in Hunfeld et al.[21] There were no statistically significant differences in baseline demographic characteristics between survivors and non-survivors. All patients were managed with a similar post-ROSC strategy according to the Dutch national guideline for pediatric post-CA care, which is based on the contemporary ERC post-ROSC guidelines.

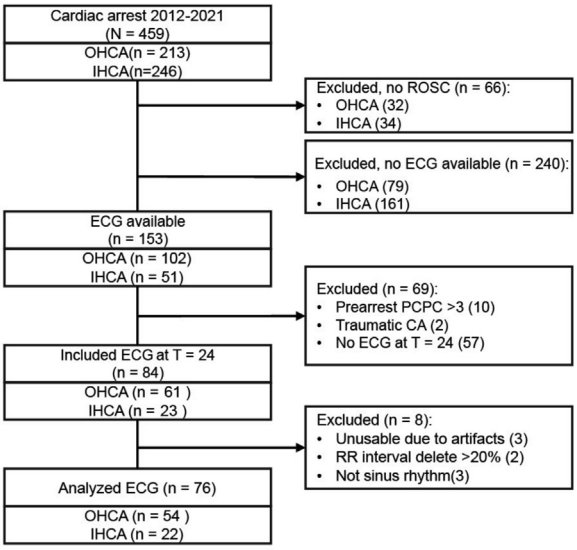

Fig. 1 – Flowchart of patient inclusion and exclusion criteria. This flow chart illustrates the patient population screened for inclusion in our study and reasons for exclusion.
IHCA in-hospital cardiac arrest; OHCA out of hospital cardiac arrest; ROSC return of spontaneous circulation.

Comparisons of HRV parameters between survival and non-survival groups

As shown in Table 2, all included HRV features at 24 h after CA except pNN50 and relative LF power showed significant differences between survivors and non-survivors (all $p < 0.05$). The time-domain parameters were significantly higher in the survival group, including SDNN (9.8 vs 3.1 ms, $p < 0.001$) and RMSSD (4.8 vs 3.3 ms, $p = 0.005$), compared to the non-survival group.

For the frequency-domain HRV indices, the absolute power spectrum parameters were significantly higher in the survival group, including total power (80.7 vs 2.2 ms^2, $p < 0.001$), VLF power (48.8 vs 0.7 ms^2, $p < 0.001$), LF power (7.6 vs 0.2 ms^2, $p < 0.001$), and HF power (4.0 vs 0.5 ms^2, $p < 0.001$). However, relative to the VLF and LF components, the proportion of HF was significantly lower in the survival group, with lower relative HF power (7.7 vs 23.8%, $p < 0.001$) and HF norm (30.1 vs 73.2, $p < 0.001$), alongside higher LF/HF ratios (2.3 vs 0.4, $p < 0.001$).

All nonlinear parameters were significantly higher in the survival group, including SD1, SD2, the SD2/SD1 ratio, sample entropy, and both DFA components.

The relationships of VIS with outcome and HRV parameters

Among the 20 patients (25.0%) with available VIS data, non-survivors tended to have higher VIS than survivors (median [IQR]: 63.9 [15.0–99.7] vs 10.1 [3.8–29.2]), but didn't reach statistical significance ($p = 0.056$, Additional file 1: Fig. S1A). Correlation analysis showed no links between VIS and time-domain HRV parameters, while significant moderate associations were found with frequency-domain parameters like VLF power ($r = -0.49$, $p = 0.028$), LF power ($r = -0.46$, $p = 0.042$), Total power (-0.50, $p = 0.024$), and relative HF power ($r = 0.51$, $p = 0.022$). Also, moderate correlations with DFA

Table 1 – Patient's characteristics. Data are presented as n (%) or median [interquartile range]. Abbreviations: CA cardiac arrest; SIDS sudden infant death syndrome.

Patient's characteristics	Total (*N* = 76)	Survive (*N* = 34)	Death (*N* = 42)	P-value
Age, (years)	2.5 [0.4–8.0]	2.5 [0.5, 7.7]	3.0 [0.4, 8.8]	0.884
Male sex, N (%)	48 (63.2)	22 (64.7)	26 (61.9)	0. 990
CA location, N (%)				0.176
In-hospital	22 (28.9)	13 (38.2)	9 (21.4)	
Out-of-hospital	54 (71.1)	21 (61.8)	33 (78.6)	
Cause of arrest, N (%)				0.056
Drowning	16 (21.1)	10 (29.4)	6 (14.3)	
Circulatory failure	15 (19.7)	8 (23.5)	7 (16.7)	
Respiratory failure	8 (10.5)	2 (5.9)	6 (14.3)	
Airway obstruction	7 (9.2)	4 (11.8)	3 (7.1)	
SIDS	6 (7.9)	1 (2.9)	5 (11.9)	
Strangulation	6 (7.9)	1 (2.9)	5 (11.9)	
Arrhythmia	5 (6.6)	5 (14.7)	0 (0.0)	
Septic shock	4 (5.3)	2 (5.9)	2 (4.8)	
Unknown	6 (7.9)	0 (0.0)	6 (14.3)	
Other	3 (3.9)	1 (2.9)	2 (4.8)	
Cause of death, N (%)				
Neurological			35 (83.3)	
Cardiac			4 (9.5)	
Other			3 (7.1)	

(α1) and DFA (α2) were observed. A strong correlation was observed with SD2/SD1 ($r = -0.71$, $p < 0.001$). In terms of prognostic prediction value, higher VIS demonstrated a moderate correlation with higher predicted probability of non-survival ($r = 0.56$, $p = 0.01$) (Additional file 1: Table S1); however, clinical outcome heterogeneity was observed: among patients with VIS < 20, 50% (5/10) of patients still experienced unfavorable outcomes (Additional file 1: Fig. S1B).

Model evaluation and feature importance analysis

Based on the HRV parameters, a random forest model was trained to predict death after 12 months, achieving an AUC of 0.85 (Fig. 2), with an accuracy of 0.78. Out of the 33 patients where the model predicted an unfavorable outcome, 29 were no longer alive after 12 months (precision of 0.88). However, the model's ability to predict survival was less robust, as 13 of 43 patients predicted to have a good outcome experienced unfavorable outcomes (negative predictive value of 0.80). The model achieved a recall of 0.69 by correctly identifying 29 out of 42 deceased patients. The overall F1-score was 0.77.

We conducted a SHAP analysis to evaluate the feature importance for our model predictions (Fig. 3A). The SHAP values revealed that the most important feature was total power followed by VLF power, SD2and DFA(α1). The beeswarm summary plot demonstrates the impact of various feature values on the model's prediction (Fig. 3B). Lower values of total power, VLF power, SD2, DFA(α1), and LF power are associated with a higher predicted probability of mortality following CA. Distinct trends in the SHAP value distribution reveal clear differences in the model's pathways for predicting survival and death (Fig. 3C).

SHAP dependence plots

In Fig. 4, the SHAP dependence plots and outcome-based feature distributions indicate critical threshold values that effectively distinguished shifts in model output contribution and reasonably separate actual outcomes for the two most important features of the model. VLF power showed positive SHAP values (contribution to prediction of unfavorable outcomes) below 2.2 ms^2, indicating lower VLF power

Table 2 – Comparison of HRV parameters between survival and non-survival group at 24 h after CA. Data are presented as n (%) or median [interquartile range]. P-values were corrected for multiple testing using the False Discovery rate (FDR) method. Abbreviations: HRV heart rate variability; RMSSD square root of the mean of the squares of differences between adjacent RR intervals; SDNN standard deviation of all RR intervals; VLF very-low frequency; LF low frequency; HF high frequency; LF rel relative LF power; HF rel relative HF power; LF norm normalized LF power; HF norm normalized HF power; LF/HF ratio of low- to high-frequency power, pNN50% of successive RR intervals differing >50 ms, SD1 and SD2 standard deviations of short and long axis of Poincaré plot, DFA detrended fluctuation analysis.

HRV parameters	Survival	Non-survival	P-value
RMSSD (ms)	4.8 [3.7–12.0]	3.3 [2.9–6.2]	0.005
SDNN (ms)	9.8 [6.0–14.0]	3.1 [2.1–5.2]	<0.001
pNN50 (%)	0.0 [0.0–0.4]	0.0 [0.0–0.2]	0.362
VLF power (ms^2)	48.8 [9.3–91.0]	0.7 [0.3–4.1]	<0.001
LF power (ms^2)	7.6 [2.3–43.5]	0.2 [0.1–0.9]	<0.001
HF power (ms^2)	4.0 [0.7–13.3]	0.5 [0.2–1.6]	<0.001
Total power (ms^2)	80.7 [18.9–210.5]	2.2 [1.1–10.0]	<0.001
VLF rel (%)	57.0 [40.0–68.1]	38.1 [26.3–56.3]	0.003
LF rel (%)	16.2 [7.1–25.7]	9.9 [5.2–19.1]	0.056
HF rel (%)	7.7 [2.9–18.9]	23.8 [11.1–41.3]	<0.001
LF norm	69.9 [47.2–79.3]	26.8 [10.0–51.2]	<0.001
HF norm	30.1 [20.7–52.8]	73.2 [48.8–90.0]	<0.001
LF/HF	2.3 [0.9–3.8]	0.4 [0.1–1.0]	<0.001
SD1 (ms)	3.4 [2.6–8.5]	2.3 [2.0–4.4]	0.005
SD2 (ms)	13.2 [7.7–19.1]	3.3 [2.0–5.8]	<0.001
SD2/SD1	2.5 [1.6–4.4]	1.0 [0.8–1.6]	<0.001
Sample entropy	1.1 [0.8–1.4]	0.7 [0.5–0.9]	<0.001
DFA (α1)	0.9 [0.6–1.1]	0.3 [0.2–0.5]	<0.001
DFA (α2)	1.2 [1.0–1.4]	0.8 [0.3–1.1]	<0.001

levels correlated with higher model-predicted mortality risk (Fig. 4A). Notably, Of the 31 individuals with VLF power below this threshold, 29 (93.5%) died (Fig. 4B). Total power exhibited similar patterns showing a shift toward positive SHAP values and high mortality below 14.3 ms^2, with 26 out of 42 individuals (85.7%) deceased (Fig. 4C and D). The results indicate that values of the two features below their respective thresholds are associated with increased risk of mortality.

Discussion

In this retrospective study, the prognostic value of HRV parameters for predicting 12-month survival outcome after CA in 76 pediatric patients was investigated. The results demonstrated that all the HRV parameters except pNN50, relative HF power and HF norm were significantly lower at 24 h after cardiac arrest in the non-survivor compared to the survivor group. A random forest model developed based on these HRV parameters (including time-domain, frequency-domain, and non-linear analyses) achieved high predictive performance and specificity in predicting unfavorable outcome, with total power and VLF power being the most informative predictors during SHAP analysis. These findings suggest the prognostic potential of HRV-based machine learning models in pediatric CA patients, as well as their potential role in supporting clinical decision-making.

In the context of pediatric CA prognosis, false-positive predictions may lead to the premature withdrawal of treatment in potentially sur-

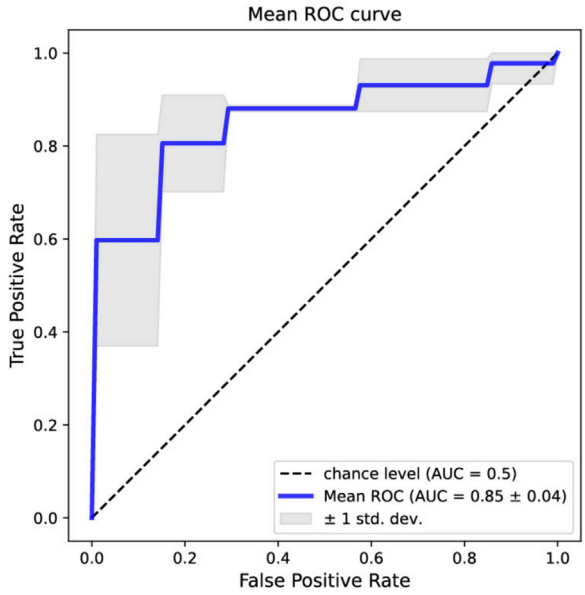

Fig. 2 – Random forest model performance using HRV features for 12-month mortality prediction.
An average area under the curve (AUC) of 0.85 (± standard deviation shown in gray) was observed across five training folds, indicating strong predictive performance. ROC receiver-operating characteristic.

vivable patients, resulting in irreversible decisions that impact the potential chances of survival. To reduce these risks, a conservative mortality prediction threshold of 0.7 was applied, which may contribute to a modest decline in the negative predictive value.

Frequency-domain parameters and non-linear domain HRV parameters contributed significantly to prediction of the model, with the top four predictive features being total power, VLF power, SD2 and DFA (α1). The HF component of the HRV spectrum mainly reflects parasympathetic modulation of the heart rate while the LF component is influenced by both sympathetic and parasympathetic nervous systems. The physiological mechanisms underlying VLF are less clearly understood and more complex than LF and HF bands since it is influenced by various long-term and complex physiological regulations and cannot be directly verified in the short term. Evidence indicates that the VLF activity is produced by the intrinsic cardiac rhythm and could be modulated by ANS activity, with early evidence suggesting that increased sympathetic activity significantly elevates the intrinsic VLF rhythm.[28] However, Talor et al. reported that β-adrenergic blockade did not significantly alter VLF power, suggesting a limited role for sympathetic regulation. In contrast, parasympathetic blockade can almost completely abolish the VLF power, indicating a critical role of parasympathetic innervation in VLF regulation.[29] Moreover, the renin-angiotensin system[30] and inflammatory responses[31] are also involved in the modulation of the VLF rhythm. Consequently, changes in VLF power may reflect the systemic functional status, supporting its utility as a prognostic indicator in severe conditions like CA. Total power comprises the powers in all HRV frequency bands (including VLF) and serves as an essential indicator of the modulation capacity of the ANS. Decreased total power is closely related to increased mortality, thus playing a critical role in risk stratification and prognosis.[32]

SD2 and DFAα1 are nonlinear indices of HRV. SD2 reflects long-term HRV and the overall activity of the ANS. A decreased SD2 is observed in CA adult patients with poor prognosis,[33] whereas elevated SD2 is associated with improved prognosis in patients with heart failure,[34] indicating the important prognostic role of SD2.The final top feature, DFA α1, reflects the autocorrelation properties of heart rate time series over short time scales. Compared to conventional time- and frequency-domain HRV measures, DFA α1 is more sensitive to changes in the cardiac dynamic structure and demonstrates greater robustness,[35] making it a valuable source of incremental prognostic information.[36] Particularly in conditions like myocardial infarction and arrhythmias, it shows stronger predictive capacity for mortality than conventional linear measurements.[37]

Consistent with our findings, Benghanem et al. also observed that VLF, SD2 and DFA α1 were significantly lower in adult patients with unfavorable outcomes after CA.[33] Endoh et al. also found the strong predictive value of ln VLF and D F A(α1) for early outcomes in adult[19] Beyond these parameters, we also found that SDNN was the only time-domain feature among the model's top ten predictors. Evidence from animal models shows that both time-domain and frequency-domain parameters decreased after CA, but treatment with hypothermia preserved only the time domain measures (RMSSD and SDNN).[38,39] Taken together, these HRV parameters exhibit significant predictive potential for patients resuscitated after CA. Although HRV data collection time points, durations, and outcome evaluation points varied across studies, HRV still showed considerable prognostic value, highlighting its stability and reliability in predicting post–CA prognosis. Notably, none of these studies included pediatric patients, and the ANS in pediatric patients is still in the process of maturation, resulting in differences in autonomic regulation compared to adults. As these findings may not be directly applicable to pediatric populations, our study provides novel insights into the prognostic value of HRV in pediatric CA.

The impact of vasoactive medications on HRV has not been clearly established. Evidence from prior research suggests no significant impact of cardiovascular agents on HRV.[40] To quantify the level of vasoactive intervention, we calculated the VIS. Although VIS was not available for all patients, the randomness of this missing data suggests it remains representative. We found a low correlation between the VIS and model predictions, suggesting that the VIS score does not determine the prognosis itself. Furthermore, a limited correlation between VIS scores and the most predictive HRV features in the model was observed, indicating that HRV may offer prognostic information independent of VIS. Therefore, HRV remains associated with clinical outcomes regardless of VIS influence.

In clinical practice, HRV offers advantages such as non-invasiveness and real-time monitoring, making it suitable even for comatose patients unable to perform verbal or motor assessments. HRV enables dynamic tracking of autonomic nervous system changes. Compared to traditional techniques such as EEG and somatosensory evoked potential (SSEP), HRV monitoring is simpler and routinely available in PICU. It offers easily interpretable results, facilitating broad clinical application across various patient care. However, unlike HRV, EEG directly monitors the activity of the brain, possibly providing prognostic information on more subtle cognitive outcomes than only survival. Finally, integrating HRV with other modalities could further enhance and optimize prognostic assessment, improving the sensitivity and specificity of early outcome prediction.

A significant advantage of this study is that we created a prognostic model that utilizes a random forest classifier based on HRV for the

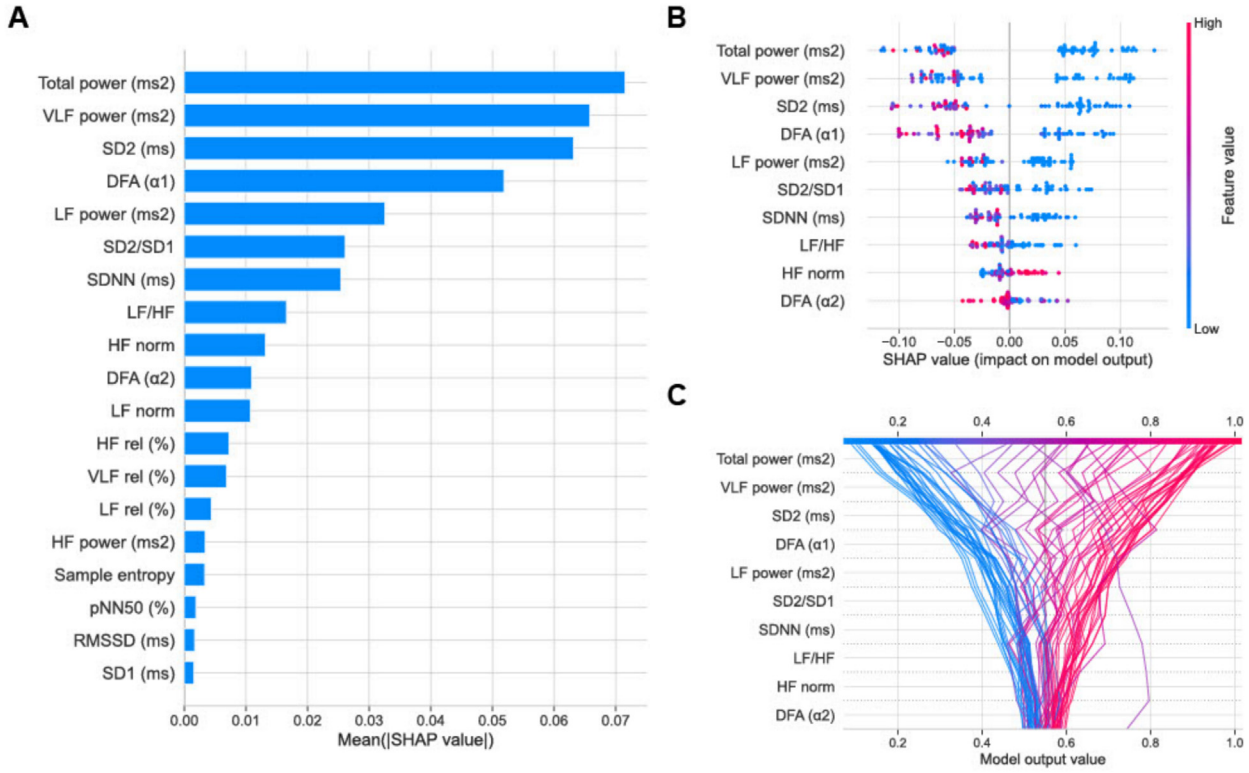

Fig. 3 – SHAP value analysis of key features in a random forest model for 12-month mortality prediction.
Panel A shows the average absolute SHAP value for each HRV feature in the random forest model. Panel B is a SHAP summary plot showing how each feature influences the prediction: High feature values are shown in red and low values in blue. A positive SHAP value means the feature pushes the prediction toward an unfavorable outcome, while a negative value indicates it supports a favorable outcome. Higher SHAP values mean the feature has a stronger impact on the model's prediction. Panel C is a decision plot that tracks how the top 10 features affect the prediction for each patient. SHAP shapley additive explanations. (For interpretation of the references to color in this figure legend, the reader is referred to the web version of this article.)

pediatric CA population. Previous research focused on the adult population. Although recent studies have utilized complex algorithms such as neural networks to construct HRV-based prediction models, the random forest model offers a significant advantage in interpretability. It can quantify the contribution of each HRV feature to the prediction of specific outcomes, which helps identify significant prognostic factors. The interpretability of the model is important, as it improves the understanding of the rationale behind each prediction, thereby supporting the development of personalized treatment plans tailored to the patient's condition. Especially, the threshold identified in the SHAP dependence plot holds significant clinical value. For instance, when VLF power is below 2.2 ms, its contribution to mortality prediction increased and a higher proportion (93.5%) of true mortality was observed, suggesting that this value may have potential for risk stratification. In clinical practice, incorporating this value into clinical assessment may enhance early recognition of high-risk children and enable earlier intensive monitoring or intervention. Unlike traditional guidelines that primarily depend on experience or retrospective data to define thresholds, this data-driven identification method may enable earlier and more personalized management and intervention strategies following resuscitation, thereby optimizing treatment outcomes.

This study has several limitations. This was a retrospective, single-center study with a limited sample size of 76 patients, restricting the generalizability of the findings. Although cross-validation was applied to reduce bias, the results require further validation in larger, multi-center cohorts. In addition, the model was trained using a binary outcome (survival vs. death) based on the PCPC score. Future studies should consider incorporating more detailed long-term neurobehavioral outcomes to offer clinicians more specific guidance and support informed decision-making. The included population is diverse in terms of CA location, etiology, and CPR duration. The added value of HRV parameters for prognostication likely differs across these variables. However, the small sample size did not allow for subgroup analysis. Previous studies have reported changes in HRV during childhood as the cardiac autonomous system matures,[41] which complicates interpretation of HRV in the PICU setting. In our cohort, we did not find a clear association with age. However, as the majority of patients were young children (median age 2.5 years, Table 1), the study was not powered to detect age-related differences in older children or adolescents. Although ECG is almost universally available in the PICU, the retrospective nature of our study limited the number of eligible patients, as older datasets were no longer accessible. This emphasizes the importance of long-term storage of clinical data, preferably in open data formats. For HRV analysis, manual inspection of 5-min RR interval windows was performed to ensure data quality and accuracy. However, according to the standards set by the European Society of Cardiology and the North American Society of Pacing and Electrophysiology, certain HRV metrics, such as SDNN, may be more

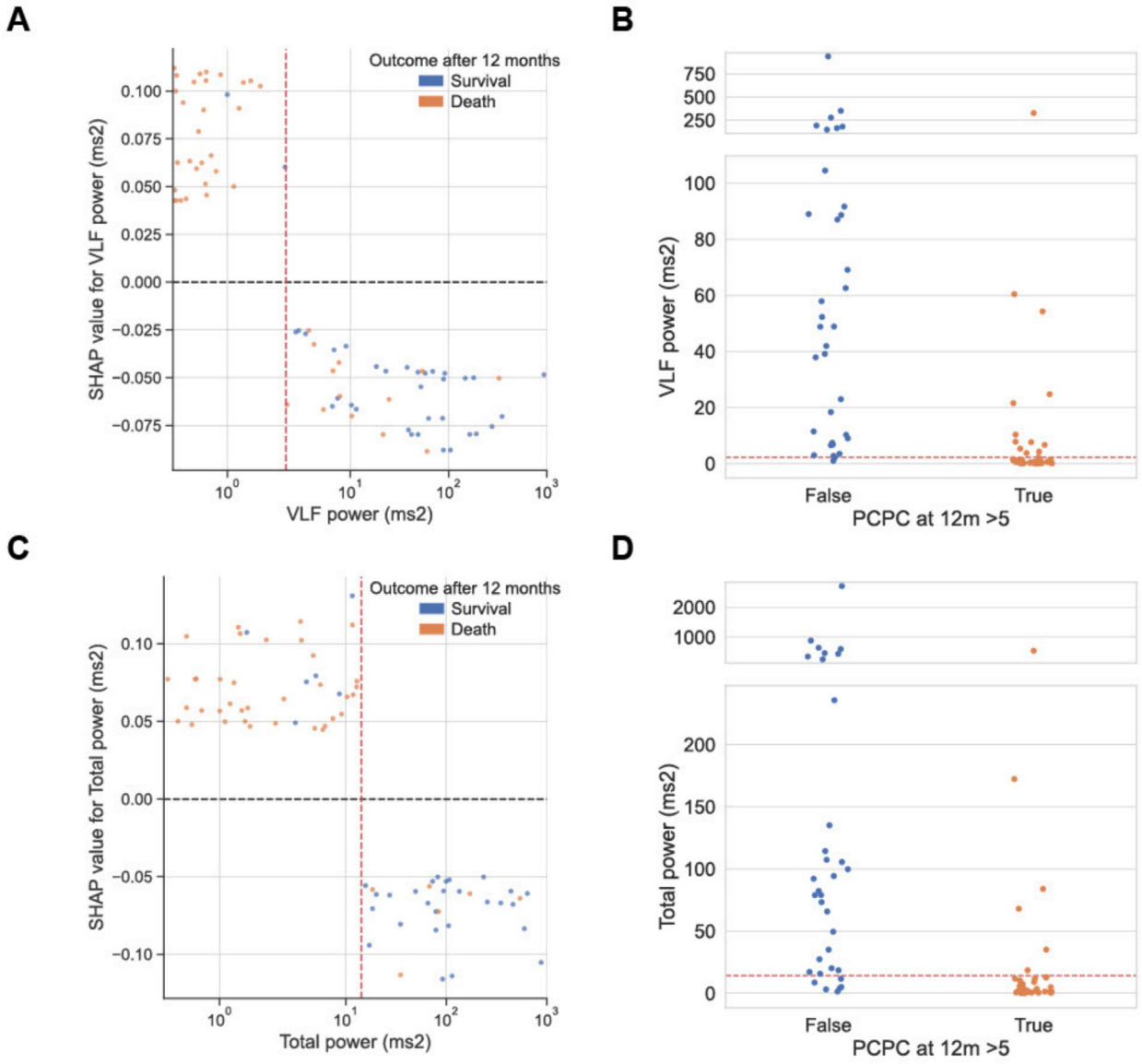

Fig. 4 – SHAP dependence plots and outcome-based feature distributions.
The dashed line at y = 0 indicates the transition point in the feature's contribution to the model's output direction; Points above contribute to a higher predicted risk of adverse outcome, while points below contribute toward a favorable outcome. The vertical red dashed line indicates the feature threshold at SHAP = 0. Point color indicates the actual clinical outcome: blue for survival and yellow for death. Panels a and c are plotted with the X-axis on a symmetric log scale. (For interpretation of the references to color in this figure legend, the reader is referred to the web version of this article.)

informative when assessed over longer recording windows,[15] Future studies may consider longer analysis durations to examine the effect of window length on HRV metric stability and predictive performance.

Conclusion

In conclusion, HRV-based machine learning models demonstrated good performance for outcome prediction in pediatric CA patients. These findings highlight the potential of HRV as a valuable tool in guiding clinical decision-making for pediatric CA patients.

Data availability

Anonymized data and code will be made available upon request from qualified investigators.

CRediT authorship contribution statement

Daishi Xu: Writing – review & editing, Writing – original draft, Formal analysis, Data curation. **Eris van Twist:** Writing – review & editing, Data curation. **Marit Verboom:** Writing – review & editing, Concep-

tualization. **Maayke Hunfeld:** Writing – review & editing, Data curation, Conceptualization. **Corinne Buysse:** Writing – review & editing. **Geurt Jongbloed:** Writing – review & editing, Methodology. **Natasja M.S. de Groot:** Writing – review & editing, Supervision. **Robert van den Berg:** Writing – review & editing, Writing – original draft, Validation, Supervision, Formal analysis, Data curation, Conceptualization.

Declaration of competing interest

The authors declare that they have no known competing financial interests or personal relationships that could have appeared to influence the work reported in this paper.

Appendix A. Supplementary material

Supplementary data to this article can be found online at https://doi.org/10.1016/j.resuscitation.2026.110983.

Author details

[a]*Department of Cardiology, Erasmus MC, University Medical Center, Rotterdam, the Netherlands* [b]*Department of Neonatal and Pediatric Intensive Care, Division of Pediatric Intensive Care, Erasmus MC Children's Hospital, Rotterdam, the Netherlands* [c]*Department of Neurology, Erasmus MC, University Medical Center, Rotterdam, the Netherlands* [d]*Delft Institute of Applied Mathematics, Delft University of Technology, the Netherlands*

REFERENCES

1. Holmberg MJ, Ross CE, Fitzmaurice GM, et al. Annual incidence of adult and pediatric in-hospital cardiac arrest in the United States. Circ Cardiovasc Qual Outcomes 2019;12:e005580.
2. Atkins DL, Everson-Stewart S, Sears GK, et al. Epidemiology and outcomes from out-of-hospital cardiac arrest in children: the Resuscitation Outcomes Consortium Epistry-Cardiac Arrest. Circulation 2009;119:1484–91.
3. Gardner MM, Morgan RW, Reeder R, et al. Trends in cardiac arrest outcomes & management in children with cardiac illness category compared to non-cardiac illness category: an analysis from the AHA Get With the Guidelines®-Resuscitation Registry. Resuscitation 2024;205:110430.
4. Girotra S, Spertus JA, Li Y, et al. Survival trends in pediatric in-hospital cardiac arrests: an analysis from Get With the Guidelines-Resuscitation. Circ Cardiovasc Qual Outcomes 2013;6:42–9.
5. Fink EL, Prince DK, Kaltman JR, et al. Unchanged pediatric out-of-hospital cardiac arrest incidence and survival rates with regional variation in North America. Resuscitation 2016;107:121–8.
6. Topjian AA, de Caen A, Wainwright MS, et al. Pediatric post–cardiac arrest care: a scientific statement from the American Heart Association. Circulation 2019;140:e194–233.
7. Lemiale V, Dumas F, Mongardon N, et al. Intensive care unit mortality after cardiac arrest: the relative contribution of shock and brain injury in a large cohort. Intensive Care Med 2013;39:1972–80.
8. Nolan JP, Berg RA, Callaway CW, et al. The present and future of cardiac arrest care: international experts reach out to caregivers and healthcare authorities. Intensive Care Med 2018;44:823–32.
9. Endisch C, Westhall E, Kenda M, et al. Hypoxic-ischemic encephalopathy evaluated by brain autopsy and neuroprognostication after cardiac arrest. JAMA Neurol 2020;77:1430–9.
10. Perego C, Fumagalli F, Motta F, et al. Evolution of brain injury and neurological dysfunction after cardiac arrest in the rat – a multimodal and comprehensive model. J Cereb Blood Flow Metab 2024;44:1316–29.
11. Benghanem S, Mazeraud A, Azabou E, et al. Brainstem dysfunction in critically ill patients. Crit Care 2020;24:5.
12. Sandroni C, Cariou A, Cavallaro F, et al. Prognostication in comatose survivors of cardiac arrest: an advisory statement from the European Resuscitation Council and the European Society of Intensive Care Medicine. Resuscitation 2014;85:1779–89.
13. Hunfeld M, Ketharanathan N, Catsman C, et al. A systematic review of neuromonitoring modalities in children beyond neonatal period after cardiac arrest*. Pediatr Crit Care Med 2020;21:e927.
14. Ahn JH, Lee TK, Tae HJ, et al. Neuronal death in the CNS autonomic control center comes very early after cardiac arrest and is not significantly attenuated by prompt hypothermic treatment in rats. Cells 2021;10:60.
15. Camm AJ, Malik M, Bigger JT, et al. Heart rate variability. Standards of measurement, physiological interpretation, and clinical use. Task Force of the European Society of Cardiology and the North American Society of Pacing and Electrophysiology. Eur Heart J 1996;17:354–81.
16. Buchman TG, Stein PK, Goldstein B. Heart rate variability in critical illness and critical care. Curr Opin Crit Care 2002;8:311.
17. Kwon SB, Megjhani M, Nametz D, Agarwal S, Park S. Heart rate and heart rate variability as a prognosticating feature for functional outcome after cardiac arrest: a scoping review. Resusc Plus 2023;15:100450.
18. Pfeifer R, Hopfe J, Ehrhardt C, Goernig M, Figulla HR, Voss A. Autonomic regulation during mild therapeutic hypothermia in cardiopulmonary resuscitated patients. Clin Res Cardiol 2011;100:797–805.
19. Endoh H, Kamimura N, Honda H, Nitta M. Early prognostication of neurological outcome by heart rate variability in adult patients with out-of-hospital sudden cardiac arrest. Crit Care 2019;23:323.
20. Chen WL, Tsai TH, Huang CC, Chen JH, Kuo CD. Heart rate variability predicts short-term outcome for successfully resuscitated patients with out-of-hospital cardiac arrest. Resuscitation 2009;80:1114–8.
21. Hunfeld M, Verboom M, Josemans S, et al. Prediction of survival after pediatric cardiac arrest using quantitative EEG and machine learning techniques. Neurology 2024;103:e210043.
22. Bota P, Silva R, Carreiras C, Fred A, da Silva HP. BioSPPy: a Python toolbox for physiological signal processing. SoftwareX 2024;26:101712.
23. Shaffer F, Ginsberg JP. An overview of heart rate variability metrics and norms. Front Public Health 2017;5:258.
24. Gomes P, Margaritoff P, Plácido da Silva H. pyHRV: development and evaluation of an open-source python toolbox for heart rate variability (HRV). In: Silver Lake, Serbia. p. 822–8.
25. Sandrio S, Krebs J, Leonardy E, Thiel M, Schoettler JJ. Vasoactive inotropic score as a prognostic factor during (cardio-) respiratory ECMO. J Clin Med 2022;11:2390.
26. Pedregosa F, Varoquaux G, Gramfort A, et al. Scikit-learn: machine learning in python. J Mach Learn Res 2011;12:2825–30.
27. Lundberg SM, Erion G, Chen H, et al. From local explanations to global understanding with explainable AI for trees. Nat Mach Intell 2020;2:56–67.
28. Shaffer F, McCraty R, Zerr CL. A healthy heart is not a metronome: an integrative review of the heart's anatomy and heart rate variability. Front Psychol 2014;5:1040.
29. Taylor JA, Carr DL, Myers CW, Eckberg DL. Mechanisms underlying very-low-frequency RR-interval oscillations in humans. Circulation 1998;98:547–55.
30. Akselrod S, Gordon D, Ubel FA, Shannon DC, Berger AC, Cohen RJ. Power spectrum analysis of heart rate fluctuation: a quantitative

probe of beat-to-beat cardiovascular control. Science 1981;213:220–2.
31. Stein PK, Barzilay JI, Chaves PHM, et al. Higher levels of inflammation factors and greater insulin resistance are independently associated with higher heart rate and lower heart rate variability in normoglycemic older individuals: the Cardiovascular Health Study. J Am Geriatr Soc 2008;56:315–21.
32. Aronson D, Mittleman MA, Burger AJ. Measures of heart period variability as predictors of mortality in hospitalized patients with decompensated congestive heart failure. Am J Cardiol 2004;93:59–63.
33. Benghanem S, Sharshar T, Gavaret M, et al. Heart rate variability for neuro-prognostication after CA: insight from the Parisian registry. Resuscitation 2024;202:110294.
34. Shi Y, Zhang X, Ma C, et al. Dynamic HRV monitoring and machine learning predict NYHA improvements in acute heart failure patients. Comput Biol Med 2025;189:109995.
35. Gronwald T, Hoos O. Correlation properties of heart rate variability during endurance exercise: a systematic review. Ann Noninvasive Electrocardiol 2019;25:e12697.
36. Perkiömäki JS, Mäkikallio TH, Huikuri HV. Fractal and complexity measures of heart rate variability. Clin Exp Hypertens 2005;27:149–58.
37. Mahon NG, Hedman AE, Padula M, et al. Fractal correlation properties of R-R interval dynamics in asymptomatic relatives of patients with dilated cardiomyopathy. Eur J Heart Fail 2002;4:151–8.
38. Doulalas AD, Flather MD, Pipilis A, et al. Evolutionary pattern and prognostic importance of heart rate variability during the early phase of acute myocardial infarction. Int J Cardiol 2001;77:169–79.
39. Li Y, Ristagno G, Guan J, et al. Preserved heart rate variability during therapeutic hypothermia correlated to 96 hrs neurological outcomes and survival in a pig model of cardiac arrest*. Crit Care Med 2012;40:580.
40. van der Laan L, van Wijk RJ, Quinten VM, Bouma HR, ter Maaten JC. The effect of cardiovascular medication on heart rate variability in patients presenting with early sepsis at the emergency department: a prospective cohort study. SN Compr Clin Med 2024;6:30.
41. Harteveld LM, Nederend I, ten Harkel ADJ, et al. Maturation of the cardiac autonomic nervous system activity in children and adolescents. J Am Heart Assoc 2021;10:e017405.